Optical refrigeration to 119 K, below National Institute of Standards and Technology cryogenic temperature

Seth D. Melgaard,[1,*] Denis V. Seletskiy,[1,3,4] Alberto Di Lieto,[2] Mauro Tonelli,[2] and Mansoor Sheik-Bahae[1]

[1]*University of New Mexico, Physics and Astronomy Dept., 800 Yale Blvd. NE, Albuquerque, New Mexico 87131, USA*

[2]*NEST, Nanoscience Insitute -CNR, Dipartimento di Fisica, Universita' di Pisa, Largo B. Pontecorvo, Pisa 3-56127, Italy*

[3]*Air Force Research Laboratory, Kirtland AFB, New Mexico 87117, USA*

[4]*Currently at the Department of Physics and Center for Applied Photonics, University of Konstanz, Konstanz 78457, Germany*

**Corresponding author: melgaard@unm.edu*

Received February 20, 2013; revised April 2, 2013; accepted April 3, 2013;
posted April 8, 2013 (Doc. ID 185607); published May 1, 2013

We report on bulk optical refrigeration of Yb:YLF crystal to a temperature of ~124 K, starting from the ambient. This is achieved by pumping the E4-E5 Stark multiplet transition at ~1020 nm. A lower temperature of 119 ± 1 K ($\sim -154C$) with available cooling power of 18 mW is attained when the temperature of the surrounding crystal is reduced to 210 K. This result is within only a few degrees of the minimum achievable temperature of our crystal and signifies the bulk solid-state laser cooling below the National Institute of Standards and Technology (NIST)-defined cryogenic temperature of 123 K. © 2013 Optical Society of America

OCIS codes: (000.6850) Thermodynamics; (140.3320) Laser cooling; (160.5690) Rare-earth-doped materials; (300.1030) Absorption; (300.2530) Fluorescence, laser-induced.
http://dx.doi.org/10.1364/OL.38.001588

During optical refrigeration of a solid, heat is removed by the process of anti-Stokes fluorescence [1–3], when the average emission energy exceeds the excitation energy. The energy difference is extracted from the phonon modes of that solid, resulting in cooling of the lattice. Since the first observation of laser cooling of ytterbium-ion-doped glass in 1995 [2], a variety of Yb-ion:host combinations have been cooled (for a comprehensive list, see recent review articles [4,5]). In addition, cooling with rare-earth ions of thulium [6] and erbium [7] has been demonstrated. Optical refrigeration has also motivated the development of a radiation-balanced laser [8].

Cooling to 155 K was recently achieved in the Yb^{3+}:$LiYF_4$ crystal by 0.3% detuned excitation from the optimal pump energy, corresponding to the lowest Stark intermultiplet resonance (E4-E5) [9]. For ideal pumping, a minimum achievable temperature (MAT) of 110 K was predicted [9] and verified spectroscopically [10] for a given level of material purity.

In this Letter we report on bulk laser cooling to (119 ± 1) K of the 5% w.t. Yb:YLF crystal, pumped directly at the lowest energy intermultiplet E4-E5 transition at $\lambda = 1020$ nm. This temperature is the coldest achieved by any all-solid-state refrigerator to date and corresponds to the first bulk cooling below the National Institute of Standards and Technology (NIST)-defined cryogenic temperature of 123 K. Furthermore, cooling to within few degrees from the MAT signifies excellent agreement with the modeling framework.

A description of realistic materials for laser cooling has to take into account the competing, heat generating, loss terms. The main losses are nonradiative recombination and impurity-mediated heating. Thus, the necessary material conditions to achieve cooling are (i) high external quantum efficiency (EQE) transition in the dopant ion and (ii) high purity of the host material. Ignoring saturation [11], the cooling efficiency, defined as the ratio of power heat lift to absorbed power, is given by [3,11]

$$\eta_c(\lambda, T) = \eta_{\text{ext}}\left[\frac{1}{1 + \alpha_b/\alpha(\lambda, T)}\right]\frac{\lambda}{\lambda_f(T)} - 1, \qquad (1)$$

where $\lambda_f(T)$ is a temperature-dependent mean emission wavelength, η_{ext} is the EQE, and α_b, $\alpha(\lambda, T)$ are the parasitic and resonant absorption coefficients, respectively; the latter is shown to be explicitly wavelength- and temperature dependent. While the nature of the background absorption is under current investigation, a widely accepted view is that it is mainly due to transition metal impurities [12]. Both η_{ext} and α_b are assumed to be temperature independent, justified in earlier local cooling measurements of the MAT [10]. In Eq. (1), a positive value of η_c corresponds to cooling, where a small ratio of α_b/α together with a high value of η_{ext} are the necessary requirements.

To calculate the cooling efficiency of the material for moderate pumping (ignoring saturation), we have to supplement Eq. (1) with four measured values, namely η_{ext}, α_b, $\alpha(\lambda, T)$, and $\lambda_f(T)$ [11]. The latter two quantities are obtained in a series of experiments where calibrated temperature-dependent fluorescence spectra are analyzed by performing reciprocity [13] and by taking the first moment of the fluorescence function, respectively. Supplemented by the data, the cooling efficiency is calculated from Eq. (1) and plotted in Fig. 1. The blue region corresponds to cooling. The line separating the cooling from the heating (red) region is the spectrum of the MAT. The global minimum of that spectrum, denoted as MAT_g, occurs at a wavelength of 1020 nm, corresponding to the E4-E5 transition, as mentioned above. The exact MAT_g value depends on the input parameters of the model and is estimated to be 116 K for the Yb:YLF sample used in this work.

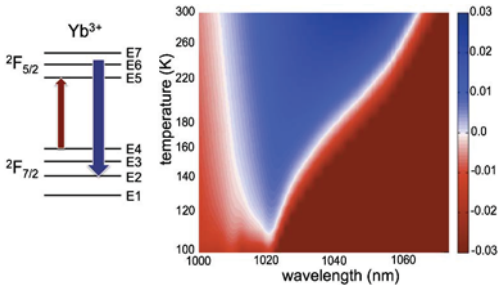

Fig. 1. (Left) The cooling cycle associated with the Stark multiplet of Yb^{3+}, showing explicitly the E4-E5 pumped transition. (Right) Map of cooling efficiency [Eq. (1)] for Yb^{3+}:YLF with $\eta_{ext} = (99.4 \pm 0.1)\%$ and $\alpha_b = (4.4 \pm 0.2 \times 10^{-4})$ cm^{-1}.

To reach optimal pumping conditions, we acquired a custom-designed linearly polarized high-power (>50 W) Yb:fiber laser at 1020 nm from IPG Photonics. The experimental setup is outlined in Fig. 2. The laser is optically isolated from and focused via a lens pair to a nonresonant cavity that is placed inside a high vacuum chamber. To maximize single-pass absorption [14] and minimize surface reflections, the Yb:YLF crystal is Brewster cut for the $E\|c$ orientation. To further maximize pump absorption, crystal of length $L = 1.2$ cm is positioned inside of a Herriott cell [15], consisting of highly reflective flat input coupler and a curved ($R = 25$ cm) back mirror, separated by ~3.5 cm. Saturation of resonant absorption is avoided inside the Herriot cell by optimizing the lens pair separation and focusing spot size at the flat mirror. Pump light is admitted through a 1 mm diameter hole in the input coupler, resulting in five roundtrip passes through the crystal. Unabsorbed pump light exits the 1 mm hole, misaligned from the incident pump, to be dumped externally.

To reach cryogenic temperatures, the heat load on the cooling medium has to be minimized. This is accomplished by placing the sample into a tightly fit copper clamshell structure, which is coated inside with a low thermal emissivity material that is also highly absorbing at the fluorescence wavelengths [16]. The crystal surface area and thus the thermal load are also minimized by mode matching a cross section of the sample (3 mm × 4 mm) to the small laser mode inside of a multipass cavity. Crystal is mechanically supported by six optical fibers protruding from the clamshell walls, thus minimizing the adverse conductive heat load. The sample temperature is measured from the calibrated changes of the temperature-dependent fluorescence spectrum, using a noncontact differential technique [17]. The vacuum of a main chamber is held at 10^{-6} $Torr$ and a chilled

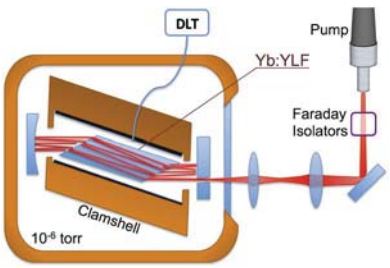

Fig. 2. Schematic of the experimental setup.

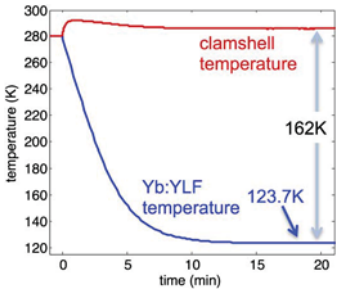

Fig. 3. Temperature evolution of Yb:YLF, from 285 K down to the NIST-defined cryogenic operation point of 123 K.

water loop is capable of maintaining the clamshell at a constant temperature around the ambient value.

The temperature evolution of the crystal when irradiated with 45 W of the pump power is shown in Fig. 3. A steady-state temperature of (123.7 ± 1.0) K was reached with an estimated ~18 W of absorbed power at 1020.70 ± 0.25 nm. This result was accomplished while keeping the clamshell temperature around 285 K. A cooling power of 50 mW was estimated at the steady state, which, within our experimental uncertainty, corresponds to the NIST-defined cryogenic temperature. A power-dependent red shift of the pump wavelength by 0.7 nm at the maximum pump power increases the MAT to 118 K, in comparison with targeted the MAT_g of 116 K as per Fig. 1.

Next, we performed a power-scaling study of the steady-state temperature, as shown in Fig. 4. The condition of equilibrium in the cooling dynamics is reached when the cooling power P_{cool} becomes equal to the load power P_{load} on the sample at a temperature T. For the dominant radiative load, this condition is given by

$$\eta_c(\lambda, T) P_{abs}(\lambda, T) = \kappa(T_c^4 - T^4), \tag{2}$$

where P_{abs} is the absorbed power, κ is a proportionality constant given by the product of a Stefan–Boltzmann constant and a geometry- and emissivity-dependent coefficient [18], and T_c is the temperature of the clamshell. The data of Fig. 4 is fit by a solid line, using Eq. (2) and η_c values from the spectroscopic measurements described above. Very good agreement is found between the measurements and the data-assisted model. In particular, the expected asymptotic behavior of the measured temperature with increasing absorbed power,

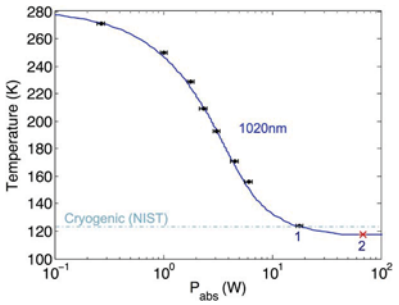

Fig. 4. Steady-state temperature scaling with the absorbed power (black), model prediction (blue line), and lowest temperature achieved by effective scaling of the absorbed power (red "x").

approaching the MAT value of 118 K, is clearly observed. The achieved temperature also indicates that saturation is avoided [11].

To reach temperatures even closer to the MAT value, either a further increase in absorbed power (P_{abs}) or an equivalent decrease in the parasitic load (P_{load}), is required [Eq. (2)]. Figure 4 shows a need for >70 W of absorbed power to reach the MAT, exceeding our currently available pump power. Limited by pump power, a proof-of-principle experiment using the latter approach is performed by modifying the water chiller feedthrough to accept liquid nitrogen, which was used to reduce the clamshell temperature T_c.

When the clamshell temperature was lowered to 208 K, a new steady state of 118.7 ± 1 K was obtained, reaching MAT of 118 K (within experimental uncertainty) for the slightly detuned pump at 1020.7(±0.25) nm (note at 1020 nm, MAT is 116 K). Further reduction of heat load did not effect the final temperature, verifying MAT. Importantly, cooling was still accomplished by all-optical means and cryogen was used only after the sample had reached its equilibrium temperature of 123.7 K. The new steady state can be projected onto the dataset obtained with the old T_c value of 285 K (Fig. 4). For that, we estimate a factor of ~3.8 reduction of the thermal load on the sample, when going from the old to the new value of the T_c. This factor is given by the corresponding ratio of the heat loads $(285^4 - 123.7^4)/(208^4 - 123.7^4)$, as per Eq. (2). The reduction of the heat load is equivalent to an effective increase of the absorbed power by the same factor, if the sample and clamshell temperatures were 123.7 and 285 K, respectively. Thus, the final temperature of 118.7 K can also be reached with an effective increase of the absorbed power by a factor ~3.4, the value lowered from the initial 3.8 estimate by the reduction of the absorption coefficient at the corresponding temperatures. In projecting the point of 118.7 K cooling, indicated by "x," onto Fig. 4, a very good agreement is found with the model prediction. We estimate laser cooling power of 18 mW at this temperature; the small value is a direct consequence of the approach to the MAT condition. For comparison, cooling power of ~630 mW is available at room temperature.

In summary, this work demonstrates a new milestone in the field of laser cooling of solids. An absolute temperature of 123.7 ± 1 K with an estimated 50 mW of heat lift has been achieved at the E4-E5 Stark resonance of Yb ions, consistent with earlier model predictions and spectroscopic measurements. This represents a new record in optical refrigeration, and is the first demonstration of bulk laser cooling of solids below a NIST cryogenic temperature of 123 K. As a proof of principle, we have also shown that a temperature of 118.7 K, only 0.7 deg above the MAT, can be reached upon further optimization.

This work was supported by an AFOSR Multi-University Research Initiative, grant No. FA9550-04-1-0356, entitled Consortium for Laser Cooling in Solids. D. V. S. acknowledges the support of a National Research Council Research Associateship Award at the Air Force Research Laboratory as well as partial support by the National Science Foundation Fellowship under award No. 1160764.

References

1. P. Pringsheim, Zeitschrift für Physik **57**, 739 (1929).
2. R. Epstein, M. Buchwald, B. Edwards, T. Gosnell, and C. E. Mungan, Nature **377**, 500 (1995).
3. M. Sheik-Bahae and R. Epstein, Nat. Photonics **1**, 693 (2007).
4. R. Epstein and M. Sheik-Bahae, *Optical Refrigeration* (Wiley-VCH, 2009).
5. G. Nemova and R. Kashyap, Rep. Prog. Phys. **73**, 086501 (2010).
6. C. Hoyt, M. Sheik-Bahae, R. Epstein, B. Edwards, and J. Anderson, Phys. Rev. Lett. **85**, 3600 (2000).
7. J. Fernandez, A. Garcia-Adeva, and R. Balda, Phys. Rev. Lett. **97**, 033001 (2006).
8. S. Bowman, IEEE J. Quantum Electron. **35**, 115 (1999).
9. D. Seletskiy, S. Melgaard, D. Bigotta, A. di Lieto, M. Tonelli, and M. Sheik-Bahae, Nat. Photonics **4**, 161 (2010).
10. D. Seletskiy, S. Melgaard, R. Epstein, A. Di Lieto, M. Tonelli, and M. Sheik-Bahae, Opt. Express **19**, 18229 (2011).
11. D. Seletskiy, M. Hehlen, R. Epstein, and M. Sheik-Bahae, Adv. Opt. Photon. **4**, 78 (2012).
12. M. Hehlen, R. Epstein, and H. Inoue, Phys. Rev. B **75**, 144302 (2007).
13. D. McCumber, Phys. Rev. **136**, A954 (1964).
14. N. Coluccelli, G. Galzerano, L. Bonelli, A. Di Lieto, M. Tonelli, and P. Laporta, Opt. Express **16**, 2922 (2008).
15. D. Herriott, H. Kogelnik, and R. Kompfner, Appl. Opt. **3**, 523 (1964).
16. J. Thiede, J. Distel, S. Greenfield, and R. Epstein, Appl. Phys. Lett. **86**, 154107 (2005).
17. B. Imangholi, M. Hasselbeck, D. Bender, C. Wang, M. Sheik-Bahae, R. I. Epstein, and S. Kurtz, Proc. SPIE **6115**, 215 (2006).
18. C. Hoyt, M. Hasselbeck, M. Sheik-Bahae, R. Epstein, S. Greenfield, J. Thiede, J. Distel, and J. Valencia, J. Opt. Soc. Am. B **20**, 1066 (2003).